Subgrid analysis of DNS of stratified Bunsen flames

W.J.S. Ramaekers, J.A. van Oijen and L.P.H. de Goey
Eindhoven University of Technology
Eindhoven, The Netherlands

1 Introduction

Direct Numerical Simulation (DNS) is a valuable tool for development of subgrid chemistry models for Large Eddy Simulations (LES). In DNS simulations of turbulent reacting flows the high computational cost associated with the large system of stiff differential equations is prohibitive even for moderate Reynolds numbers. The Flamelet Generated Manifold (FGM) [1], also known as Flamelet Prolongated ILDM (FPI) [2], tabulates thermochemical variables originating from one-dimensional laminar flame structures: *flamelets* [3]. FGM tables composed of steady premixed flamelets have proven to be very accurate for Bunsen-type flames including heat loss effects [1] and confined triple flames [4]. This study will continue on the turbulent planar CH_4-air Bunsen flames as simulated by Vreman *et al.* [5] which is similar to flames studied by Filatyev *et al.* [6], Bell *et al.* [7], Sankaran *et al.* [8] with parameters slightly changed to enable DNS with acceptable computational requirements. The novelty of this work is the stratification along the slot-axis which allows the quantification of the influence of "non-premixedness" which is typically present in gas turbine combustion chambers.

2 FGM generation

In this study premixed flamelets have been used to generate the FGM since both Bongers *et al.* [9] and Fiorina *et al.* [10] found that they represent partially-premixed flames better than counterflow diffusion flamelets if fuel and oxidizer stream are within the flammability limits. Since the envisioned goal are simulations of high Reynolds-number turbulent flows unit Lewis numbers are assumed for all species. The equations describing this type of flamelets are given by [1]:

$$\frac{\partial \rho u}{\partial x} = 0 \tag{1a}$$

$$\frac{\partial \rho u Y_\mathrm{i}}{\partial x} = \frac{\partial}{\partial x}\left(\frac{\lambda}{c_\mathrm{p}}\frac{\partial Y_\mathrm{i}}{\partial x}\right) + \dot{\omega}_i, \qquad i \in [1, \mathrm{N_s} - 1] \tag{1b}$$

$$\frac{\partial \rho u h}{\partial x} = \frac{\partial}{\partial x}\left(\frac{\lambda}{c_\mathrm{p}}\frac{\partial h}{\partial x}\right) \tag{1c}$$

$$\rho = p_0 \overline{M} / \left(\mathcal{R}\, T\right) \tag{1d}$$

in which the low Mach-number approximation is used; h, c_p and T are related by well-tabulated polynomial description [11]. The identity $\sum Y_\mathrm{i} = 1$ closes the system of equations. All flamelet computations have been performed with the in-house flame code Chem1D using the GRI 3.0 reaction scheme [12].

Correspondence to: giel.ramaekers@gmail.com

Thermochemical parameters are mapped on two control variables: the mixture fraction Z describing mixing and the reaction progress variable $\mathcal{Y}$ describing reaction progress, viz. $\varphi = \varphi(Z, \mathcal{Y})$ in which φ can denote any thermo-chemical variable. The mixture fraction Z is defined by Bilger [13]

$$Z = \frac{2\, M_H^{-1}\left[\mathcal{Z}_H - \mathcal{Z}_{H,2}\right] + 0.5\, M_C^{-1}\left[\mathcal{Z}_C - \mathcal{Z}_{C,2}\right] - M_O^{-1}\left[\mathcal{Z}_O - \mathcal{Z}_{O,2}\right]}{2\, M_H^{-1}\left[\mathcal{Z}_{H,1} - \mathcal{Z}_{H,2}\right] + 0.5\, M_C^{-1}\left[\mathcal{Z}_{C,1} - \mathcal{Z}_{C,2}\right] - M_O^{-1}\left[\mathcal{Z}_{O,1} - \mathcal{Z}_{O,2}\right]} \tag{2}$$

in which $\mathcal{Z}$ denotes element mass fractions of respectively hydrogen (H), carbon (C) and oxygen (O) and 1 and 2 denote the fuel and oxidizer respectively. For the reaction progress variable $\mathcal{Y}$ a linear combination of species mass fractions

$$\mathcal{Y} = (1/M_{\mathrm{CO_2}})\, Y_{\mathrm{CO_2}} + (1/M_{\mathrm{H_2O}})\, Y_{\mathrm{H_2O}} + (1/M_{\mathrm{H_2}})\, Y_{\mathrm{H_2}} \tag{3}$$

has been chosen which allows unambiguous mapping of the dependent variables for the partially-premixed $\mathrm{CH_4}$-air flames which are considered in this study. The chemical equilibrium solution is explicitly added to ensure the correct equilibrium composition for slow evolving species. 600 preheated flamelets are computed between $\phi = 0.4$ and $\phi = 1.0$ with an initial temperature $T_0 = 800$ K; thermo-chemical variables are interpolated on a equidistant 201×201 Z-$\mathcal{Y}$ grid and subsequently ρ and c_{p} are recalculated. As an example temperature and progress variable source term are shown in figure 1.

3 Governing DNS equations and numerical discretization

The Navier-Stokes equations for turbulent combustion with tabulated chemistry and unit Lewis numbers for Z and $\mathcal{Y}$ read:

$$\frac{\partial \rho}{\partial t} + \frac{\partial \rho u_j}{\partial x_j} = 0 \tag{4a}$$

$$\frac{\partial \rho u_i}{\partial t} + \frac{\partial \rho u_i u_j}{\partial x_j} = \frac{\partial p}{\partial x_i} + \frac{\partial}{\partial x_j}\left[\mu\left(\frac{\partial u_i}{\partial x_j} + \frac{\partial u_j}{\partial x_i}\right) - \frac{2}{3}\mu\frac{\partial u_k}{\partial x_k}\delta_{ij}\right] \tag{4b}$$

$$\frac{\partial \rho Z}{\partial t} + \frac{\partial \rho u_j Z}{\partial x_j} = \frac{\partial}{\partial x_j}\left(\frac{\lambda}{c_{\mathrm{p}}}\frac{\partial Z}{\partial x_j}\right) \tag{4c}$$

$$\frac{\partial \rho \mathcal{Y}}{\partial t} + \frac{\partial \rho u_j \mathcal{Y}}{\partial x_j} = \frac{\partial}{\partial x_j}\left(\frac{\lambda}{c_{\mathrm{p}}}\frac{\partial \mathcal{Y}}{\partial x_j}\right) + \dot{\omega}_{\mathcal{Y}} \tag{4d}$$

where the summation convention is used over the indices j and k and a Newtonian behavior of the fluid is assumed. ρ, $\dot{\omega}_{\mathcal{Y}}$, T and c_{p} are retrieved from the FGM table using linear interpolation in both Z and $\mathcal{Y}$ direction. In this study a simplified formulation for λ and μ of $\mathrm{CH_4}$-air flames [14] are used to reduce

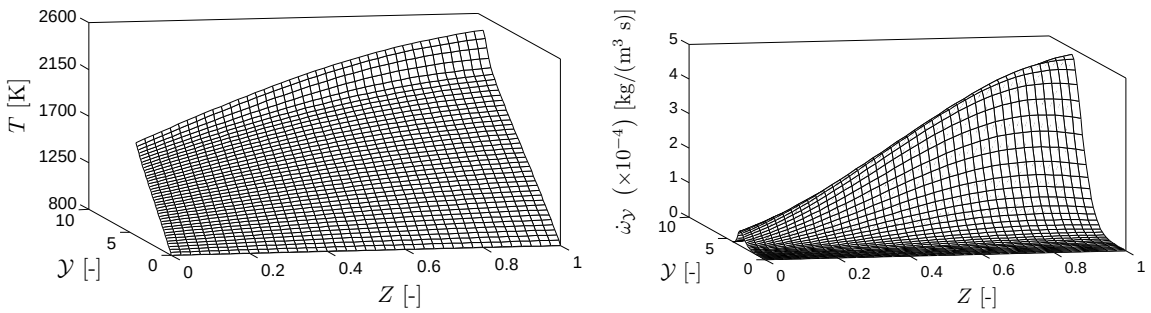

Figure 1: Temperature (left figure) and progress variable source term (right figure) as a function of Z and $\mathcal{Y}$ in the used FGM table ($\phi \in [0.4\ 1.0]$, $T_0 = 800$). Every fifth entry of both Z and $\mathcal{Y}$ is shown.

computational cost in both the flamelet equations (1) and the Navier-Stokes equations (4). A standard finite volume method is employed on a staggered Cartesian mesh. For the momentum equations second-order central differencing and an explicit hybrid timestepping method are applied: convective terms are integrated in time using a third-order Adams-Bashforth scheme while viscous terms are integrated in time using a forward Euler scheme. The central differencing ensures low numerical dissipation and the hybrid timestepping method provides better stability than than a pure Adams-Bashforth or a pure forward Euler method. For the scalars Z and $\mathcal{Y}$ the Van Leers third-order accurate MUSCL scheme is applied to the advective terms while second-order central differencing is applied to viscous terms. The variable density approach, which involves a multigrid solution method of a Poisson equation for the pressure, is thorough described in [15]. The code has been parallelized using both the MPI and OpenMP protocol.

4 Planar Bunsen flames

To serve as a reference, a premixed flame an equivalence ratio $\phi = 0.7$ is simulated first. For this ϕ the mass burning rate $m^0 = 0.611$ kg/(m^{2}s) and the flamelet flame thickness δ_0, based on the temperature increase and the maximum temperature gradient, equals 0.329 mm. A grid spacing of $2.34 \cdot 10^{-2}$ mm is used, which corresponds to $\delta_0/14$. Cells with centers $|y| = 0.5\ W$ correspond to the edge of the jet of preheated unburnt mixture; W represents the slot width which equals $W = 2.4$ mm. In the burnt co-flow, the grid was stretched slightly in the y-direction starting at $|y| = 0.8\ W$. The transition between the unburnt and burnt gas stream in terms of both progress variable and streamwise inflow velocity is described by a hyperbolic tangent function with a lengthscale equal to δ_0. Figure 2 shows the computational domain for the turbulent flames; in the inflow plane the profile for the mean streamwise velocity w (z-direction) is shown from which the slot, from which the unburnt mixture is injected into the computational domain, can clearly be identified.

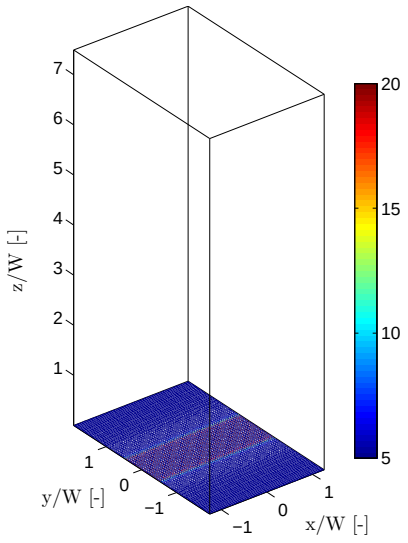

Figure 2: Computational domain for the turbulent flame simulations.

To validate the mass burning rate, a laminar flame is simulated first. The mass consumption rate is

	Laminar	Turbulent premixed	Turbulent stratified
$\overline{w}_{\text{jet}}$ / $\overline{w}_{\text{coflow}}$	20 / 5 m/s	20 / 5 m/s	20 / 5 m/s
w'_{jet} / w'_{coflow}	- / - m/s	5 / 2.5 m/s	5 / 2.5 m/s
$\Delta\phi$	-	-	0.6
$Re_{\lambda_{\text{r}}}$ $(z = W)$	-	35	34
Domain size	$0.35W \times 4W \times 8W$	$2.5W \times 4W \times 7.5W$	$2.5W \times 4W \times 7.5W$
Grid size	$36 \times 260 \times 836$	$260 \times 260 \times 772$	$260 \times 260 \times 772$

Table 1: Configurations of the simulated Bunsen flames. Domain and grid size are denoted in periodic $\times$ spanwise $\times$ streamwise direction; W denotes the slot width.

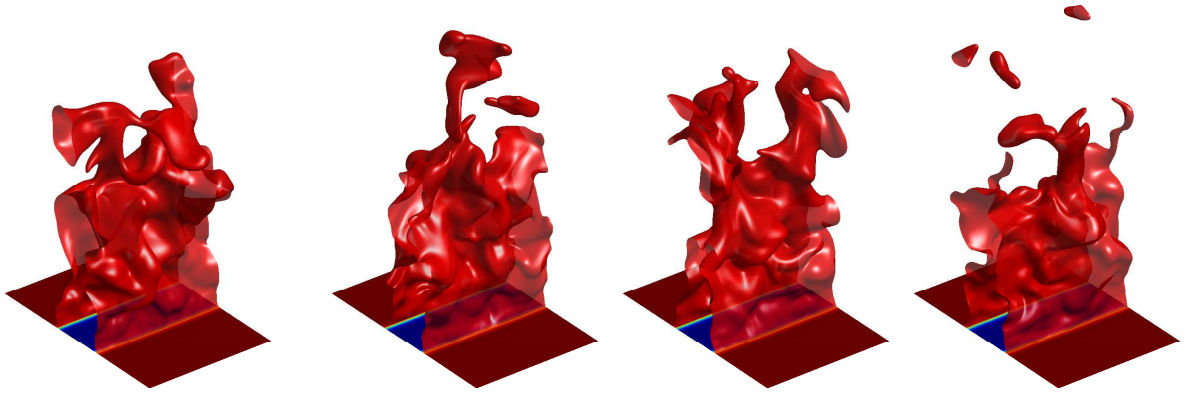

Figure 3: Subsequent snapshots of the turbulent premixed Bunsen flame with $\Delta t = 0.75$ ms.

defined by

$$m = \frac{1}{A_\mathrm{f}} \int_{A_\mathrm{in}} \rho w \left[\frac{\mathcal{Y}_\mathrm{b} - \mathcal{Y}}{\mathcal{Y}_\mathrm{b} - \mathcal{Y}_\mathrm{u}} \right] \mathrm{d}A \tag{5}$$

in which A_in denotes the inflow plane and A_f denotes the surface of an iso-$\mathcal{Y}$ contour. In this study the iso-$\mathcal{Y}$ contour at which $\dot{\omega}_\mathcal{Y}$ achieves its maximum value is chosen; this occurs at

$$\mathcal{Y}^\star = \left(\mathcal{Y} - \mathcal{Y}_\mathrm{u}\right) / \left(\mathcal{Y}_\mathrm{b} - \mathcal{Y}_\mathrm{u}\right) = 0.71 \tag{6}$$

in which $\mathcal{Y}^\star$ denotes the normalized progress variable. The obtained mass burning rate is very close to m^0: $m = 0.626$ kg/(m^{2}s). For the turbulent simulations, a constant time step of $\Delta t = 7.5 \cdot 10^{-5}$ ms is used in order to keep the CFL-number sufficiently low. The turbulent inflow conditions are created using a random noise generator: for each velocity component, every timestep random numbers are generated on the mesh one grid cell level below the inflow plane. A box-filter of $\Delta = 0.25W$ in all three spatial directions and a corresponding temporal filter are subsequently applied. The perturbation is multiplied by an appropriate factor to obtain the required inflow turbulent intensities. Instantaneous iso-surfaces $\mathcal{Y} = 0.71$ of the turbulent flame are shown in figure 3. Time-averaging of statistics was started at $t = 1.8$ ms which equals approximately two throughflow times. Statistics were taken at $t = 7.5$ ms but the simulation was continued until $t = 11.25$ ms to verify that the statistics were converged. For the premixed flame an average streamwise Kolmogorov length scale $\eta = 0.171$ mm and an average streamwise Taylor length scale $\lambda_\mathrm{T} = \sqrt{\overline{w'w'} / \overline{\left(\partial w' \,/\, \partial z\right)^2}} = 0.966$ mm are obtained over the region $z \in [0, 7W]$; it is thus verified that the numerical grid size is significantly smaller than the Kolmogorov length scale. The Karlovitz number $Ka = \left(\delta/\eta\right)^2 \approx 3.7$: according to Peters [16], the premixed flame is in the corrugated flamelet regime. Since the boundary conditions for fluid velocities for the stratified flame are identical to those of premixed flame, no significant deviation in turbulent length scales is expected. This is verified by comparison of Taylor length scale Reynolds number $Re_{\lambda_\mathrm{T}} = w'\lambda_\mathrm{T}/\nu$ at one slot width downstream of the inflow plane; for the premixed flame $Re_{\lambda_\mathrm{T}} = 35$ is found while for the stratified flame $Re_{\lambda_\mathrm{T}} = 34$ is found which are very close to each other. The configuration for the stratified flame is identical to the configuration of the premixed flame except for a variation in Z in the periodic direction:

$$\phi\left(x\right) = 0.7 - 0.3 \cos\left(\frac{2\pi x}{L_x}\right) \tag{7}$$

in which L_x denotes size of the computational domain in the periodic direction. The length scale based on the maximum gradient of Z equals 0.3328 mm is close to the flame thickness at the mean equiva-

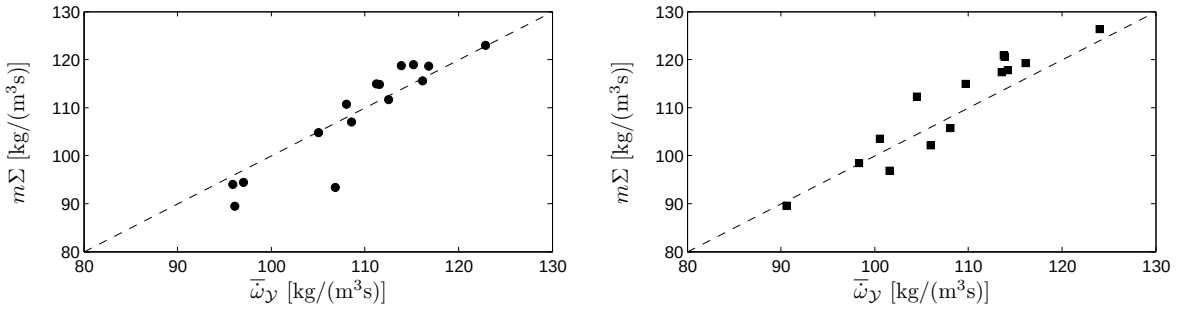

Figure 4: Comparison between the volume-averaged source term $\overline{\dot{\omega}}_{\mathcal{Y}}$ and the product of the flame surface and the (local) mass burning rate for the premixed flame (left) and the stratified flame (right).

lence ratio (0.329 mm): locally, stratification effects will thus have a significant influence on the flame structure.

5 Flame Surface Density analysis

In simulations of premixed flames, modeling of the chemical source term by a Flame Surface Density (FSD) assumption is common use. For LES applications the diffusive and chemical source contribution in equation (4d) is then replaced by:

$$\frac{\partial}{\partial x_j}\overline{\left(\frac{\lambda}{c_\mathrm{p}}\frac{\partial \mathcal{Y}}{\partial x_j}\right)} + \overline{\dot{\omega}}_{\mathcal{Y}} = \overline{m}\Sigma \tag{8}$$

in which Σ denotes the flame surface density [m^2/m^3]. For both the premixed and the stratified turbulent Bunsen flame the FSD assumption is verified in an *a priori* analysis over 15 instantaneous realizations as depicted in figure 3 for the premixed flame. For the stratified case, the mass burning rate m becomes a function of the local Z-value, viz. $m = m\left(Z\left(\vec{x}\right)\right)$; the iso-$\mathcal{Y}$ surface is taken at the same value for the normalized progress variable as for the premixed case ($\mathcal{Y}^\star = 0.71$). From the DNS results a volume averaged source term and a flame surface density source term can be extracted which are defined by

$$\overline{\dot{\omega}}_{\mathcal{Y}} = \frac{1}{V}\int_{V_\mathrm{f}} \dot{\omega}_{\mathcal{Y}} \mathrm{d}V \tag{9a}$$

$$\overline{m}_\mathrm{f}\Sigma = \frac{1}{V}\int_{A_\mathrm{f}} m\left(Z\right) \mathrm{d}A \tag{9b}$$

In figure 4 it can be seen that for both the premixed and the stratified flame the FSD assumption holds well: a maximum deviation of only 5% between $\overline{\dot{\omega}}_{\mathcal{Y}}$ and $m\Sigma$ can be observed for both flames. Apparently, the FSD assumption is also applicable to stratified flames when local variations in the mass burning rate are taken into account.

6 Remaining work

DNS results will be filtered over $\Delta_\mathrm{les} = \delta_0$ and $\Delta_\mathrm{les} = 2\delta_0$. For the FSD model, it will be examined whether subgrid variations of the mass burning rate $m = m\left(Z\right)$ can be adequately modeled using a Presumed PDF (PPDF) for Z. Simultaneously, it will be examined whether subgrid variations in $\dot{\omega}_{\mathcal{Y}}$ can be accurately modeled using a combined PPDF for Z and $\mathcal{Y}$. The most obvious choice for the PPDF is the β-PDF which is determined by a mean and variance. Finally, Large Eddy Simulations (LES) of stratified turbulent Bunsen flames will be run using both the FSD model (including subgrid closure) and

the PPDF subgrid closure method. Different modeling approaches for variances will be applied in these simulations and results will be compared to the DNS results.

Acknowledgements

This work received funding from the European Community through the project TIMECOP-AE (project AST5-CT-2006-030828). It reflects only the authors' views and the Community is not liable for any use that may be made of the information contain therein. Parallelization of the DNS code has been performed under the Project HPC-EUROPA (211437), with the support of the European Community - Research Infrastructure Action under the FP8 "Structuring the European Research Area" Program. Finally, we would like to thank the Dutch Technology Foundation (STW) under grant no. SH-178-10 and the support of NCF, the Netherlands Computing Facilities Foundation.

References

[1] J.A. van Oijen and L.P.H. de Goey. *Combust. Sci. Technol.*, 161:113–137, 2000.

[2] O. Gicquel, N. Darabiha, and D. Thevenin. *Proc. Combust. Inst.*, 28:1901–1908, 2000.

[3] N. Peters. *Prog. Energy Combust. Sci.*, 10:319–339, 1984.

[4] J.A. van Oijen and L.P.H. de Goey. *Combust. Theor. and Model.*, 8:141–163, 2004.

[5] A.W. Vreman, J.A. van Oijen, L.P.H. de Goey, and R.J.M. Bastiaans. *Flow Turbul. and Combust.*, 82:511–535, 2009.

[6] S.A. Filatyev, J.F. Driscoll, C.D. Carter, and J.M. Donbar. *Combust. Flame*, 141:1–21, 2005.

[7] J.B. Bell, M.S. Day, J.F. Grcar, M.J. Lijewinski, J.F. Driscoll, and S.A. Filatyev. *Proc. Combust. Inst.*, 31:1299–1307, 2007.

[8] R. Sankaran, E.R. Hawkes, J.H. Chen, T. Lu, and C.K. Law. *Proc. Combust. Inst.*, 31:1291–1298, 2007.

[9] H. Bongers, J.A. van Oijen, and L.P.H. de Goey. *Combust. Sci. Technol.*, 177(12):2373–2393, 2005.

[10] B. Fiorina, O. Gicquel, L. Vervisch, S. Carpentier, and N. Darabiha. *Combust. Flame*, 140:147–160, 2005.

[11] R. Kee and J. Miller. *Springer Series in Chemical Physics*, 47:196, 1986.

[12] G.P. Smith, D.M. Golden, M. Frenklach, N.W. Moriarty, B. Eiteneer, M. Goldenberg, C.T. Bowman, R.K. Hanson, S. Song, W.C. Gardiner Jr., V.V. Lissianski, and Z. Qin. Grimech 3.0 reaction mechanism. Technical report, Sandia National Laboratories, 2000.

[13] R.W. Bilger. *Combust. Flame*, 80:135–149, 1990.

[14] M.D. Smooke. *Reduced kinetic mechanisms and assymptotic approximations for methane-air flames*, pages 1–28. Springer Verlag, Berlin, 1991.

[15] A.W. Vreman, B.A. Albrecht, J.A. van Oijen, L.P.H. de Goey, and R.J.M. Bastiaans. *Combust. Flame*, 153:394–416, 2008.

[16] N. Peters. *Turbulent combustion*. Cambridge University Press, 2000.